Available online at www.sciencedirect.com
SCIENCE DIRECT®
Talanta 67 (2005) 462–471
Talanta
www.elsevier.com/locate/talanta

Challenges in quantum dot-neuron active interfacing

Natalia Gomez [a], Jessica O. Winter [a,1], Felice Shieh [a], Aaron E. Saunders [a], Brian A. Korgel [a,c,d,*], Christine E. Schmidt [a,b,c,d,*]

[a] Department of Chemical Engineering, The University of Texas at Austin, Austin, TX 78712-1062, USA
[b] Department of Biomedical Engineering, The University of Texas at Austin, Austin, TX 78712-1062, USA
[c] Texas Materials Institute, The University of Texas at Austin, Austin, TX 78712-1062, USA
[d] Center for Nano- and Molecular Science and Technology, The University of Texas at Austin, Austin, TX 78712-1062, USA

Available online 26 July 2005

Abstract

Semiconductor nanocrystal quantum dots (qdots) are now being explored in applications requiring active cellular interfaces, such as biosensing and therapeutics in which information is passed from the qdot to the biological system, or vice versa, to perform a function. These applications may require surface coating chemistry that is different from what is commonly employed for passive interface applications like labeling (i.e., thick polymer coatings such as poly(ethylene glycol) (PEG)), in which the only concern is nonspecific sticking to cells and biocompatibility. The thick insulating coatings that are generally needed for labeling are generally not suitable for active qdot-cell interface applications. There is currently little data regarding the interactions between viable cells and qdots under physiological conditions. Our initial investigations using mercaptoacetic acid-coated CdS and CdTe qdots as a simple model to interface with neuron cell surface receptors under physiological conditions uncovered two significant technological hurdles: nonspecific binding and endocytosis. Nonspecific binding can be extensive and in general there appears to be greater nonspecific binding for larger particle sizes, but this also depends sensitively on the particle surface characteristics and the type of neuron, possibly indicating a detailed relationship between particle-cell affinity and cell membrane chemistry. More importantly, qdot endocytosis occurs rapidly at physiological temperature for the different nerve cell types studied, within the first five minutes of exposure to both CdS and CdTe qdots, regardless of whether the molecular coatings specifically recognize cell surface receptors or not. As a consequence, new strategies for tagging cell surface recognition groups for long-term active interfacing with cells under physiological conditions are needed, which requires more sophisticated ligands than MAA but also the absence of thick insulating coatings.

Keywords: Cadmium sulfide nanocrystals; Neuron labeling; Nonspecific binding; Endocytosis; Ligand passivation

1. Introduction

Semiconductor nanocrystal quantum dots (qdots) have been used for biological imaging in both in vitro [1–4] and in vivo conditions [5–8]. For imaging, the main materials requirements for the qdots are water dispersibility, biocompatibility, chemical stability and robust optical properties. Chemical coatings are essential for meeting these requirements and numerous modifications of the qdot surface chemistry have been explored, including the attachment of organic layers of poly(ethylene glycol) (PEG) [6–10] and bovine serum albumin [11–13], and biocompatible and chemically functionalizable inorganic shells such as silica [1,4,14,15]. These layers can help prevent leaching of the toxic core, improve cytocompatibility, prevent nonspecific binding, and in some cases enhance the optical properties and prevent chemical degradation [12,15].

The majority of the interfaces between qdots and cells remain largely passive (i.e., not for stimulation or activation of cellular responses) and have been used to identify cellular components and track metabolic processes [16,27,35]. However, unique qdot properties, including heat production,

* Corresponding authors. Tel.: +1 512 471 1690; fax: +1 512 471 7060.
E-mail addresses: korgel@che.utexas.edu (B.A. Korgel), schmidt@che.utexas.edu (C.E. Schmidt).
[1] Present address: Center for Innovative Visual Rehabilitation, Mail Stop 151E, VA Hospital, 150 S Huntington Ave, Boston, MA 02130, USA.

0039-9140/$ – see front matter © 2005 Elsevier B.V. All rights reserved.
doi:10.1016/j.talanta.2005.06.041

creation of a dipole moment and the capacity to drive oxidation/reduction chemistry [17,18] could be exploited to manipulate cell function. Some investigators have begun using nanoparticles for these purposes. For example, gold–silica nanoshells irradiated with near-infrared light have been used to target and destroy cancer cells. CdSe nanoparticles with the capacity of recognizing and sensitizing leukemia cells have been synthesized for photodynamic therapy; and CdS qdots have been incorporated and released from chaperonins with ATP [19–21].

As in biolabeling, these efforts to direct cell function require cytocompatibility along with the capacity to target and bind specific proteins and receptor sites, and adequate chemical and photo-stability. However, in the case of active interfaces, thick coatings on the qdots may be detrimental, preventing efficient transfer of electrons, holes or heat to the cells or decreasing local electric fields associated with the qdot. Furthermore, the increase in nanocrystal diameter due to the thick surface coating could be detrimental to biomolecular machinery in the cell nucleus, as the small nuclear membrane pore size excludes objects larger than ∼20 nm [4]. Additionally, tracking of qdot-labeled proteins and their interaction with membrane receptors could be also affected since binding sites are sometimes located in pores as small as ∼2 nm [27]. Thus, "uncoated" nanocrystals will most likely be required for active interfacing applications.

Eliminating these surface layers incurs challenges such as nonspecific binding and cytotoxicity [12]. Here, we examine nonspecific binding of "bare" mercaptoacetic acid-capped CdS and CdTe qdots exposed to three different nerve cell types and report rapid endocytosis under physiological conditions. There appears to be a direct relationship between particle synthesis conditions and cellular nonspecific binding. Endocytosis occurred regardless of the surface ligand chemistry (i.e., specific or nonspecific recognition molecules). While much is known about endocytotic processes that occur for particles larger than ∼50 nm, there is currently little known about the endocytosis of nanoparticles with diameters less than 10 nm [38].

2. Materials and methods

2.1. CdS nanocrystal synthesis

Mercaptoacetic acid (MAA)-stabilized CdS qdots were synthesized via arrested precipitation in water as described previously [22]. Mercaptoacetic acid (MAA, $HOOCHCH_2SH$) (Fluka) was added to 10 mL of aqueous $CdCl_2$ (Sigma) solution. The reactant concentrations were varied systematically to modify the properties of the qdots, as summarized in Table 1. After adding MAA, the pH was raised to 4.5 by drop wise addition of 10 M NaOH, followed by further drop wise addition of 1 M NaOH to obtain a final desired pH between 5 and 11 (Table 1). 10 mL of $Na_2S{\cdot}9H_2O$ (Sigma) solution were added to this solution with rapid stirring. The solution was stirred for 4 h prior to analysis. Particles with various sizes and ligand surface coverage were obtained by varying either the pH before adding the $Na_2S{\cdot}9H_2O$ solution, the MAA concentration or the $[CdCl_2]$:$[Na_2S]$ molar ratio.

Table 1
Experimental synthesis conditions examined

Parameter	Ligand	$[CdCl_2]$ (mM)	[Ligand] (mM)	$[Na_2S]$ (mM)	pH
Control	MAA	5	55	2	7[a] 8.2[b]
Ratio	MAA	5	55	0.8–5	7[a] 8.2[b]
Ligand	MAA	5	10–500	2	7[a] 8.2[b]
pH	MAA	5	55	2	5–11[a]

[a] pH before Na_2S addition.
[b] pH after Na_2S addition held constant with addition of HCl or NaOH (1 M).

In some cases, CdS qdots were synthesized as described previously [23] with a mixture of MAA and the peptide sequence RGD (Arg-Gly-Asp), which binds specifically to integrin receptors. Acetyl-CGGGRGDS (The University of Texas Protein Microanalysis facility) was added at 0.6 mM to 10 mL of $CdCl_2$ solution (5 mM) in addition to 220 mM MAA. The pH was increased to 12 before adding 10 mL of $Na_2S{\cdot}9H_2O$ solution. Otherwise, the synthesis proceeded as described for the MAA particles.

2.2. CdTe nanocrystal synthesis

Cadmium oxide (CdO, Aldrich) precursor (0.056 g) was mixed with 0.230 g of tetradecylphosphonic acid (TDPA, Alfa Aesar) and 3.7 g of trioctylphosphine oxide (TOPO, Aldrich). In addition, a separate flask containing 0.066 g of tellurium powder (Te, Aldrich) and 2.5 mL of trioctylphosphine (TOP, Fluka) was prepared. The CdO-containing flask was degassed on a Schlenk line at 60 °C for 2 h under 300–500 mTorr of vacuum. Then, it was placed under nitrogen and heated to 340 °C. Additionally, the Te solution was attached to the Schlenk line, placed under N_2, and heated to 150 °C. When both solutions had completed heating, the temperatures were lowered to 300 °C (CdO) and 120 °C (Te), and the 10 mL of the Te solution was injected into the CdO solution, producing a black dispersion of TOPO-capped particles. The temperature was reduced to 60 °C and stirred for 30–45 min before adding 5 mL of chloroform. To create water-soluble particles, 16 mL of 0.5 M mercaptopropionic acid (MPA, Fluka) in basic methanol (pH 12) were added to 5.2 mL of the TOPO-capped particles. The temperature was reduced to 37 °C, and particles were left to stir under nitrogen overnight. Following incubation, particles were precipitated and extracted with 2-propanol. For peptide-conjugated nanocrystals an additional partial ligand exchange was performed. After drying, the MPA-capped nanocrystals were redispersed with 6 mg of

CGGGRGDS peptide dissolved in 2 mL of PBS (to 4 mM), and stirred in a N_2 atmosphere overnight to produce ligand exchange.

2.3. Cell culture and isolation

SK-N-SH neuroblastoma cells (American Type Culture Collection #HTB-11) were cultured in DMEM cell culture medium (Sigma) with 10% fetal bovine serum (FBS, Gibco) and 1% penicillin–streptomycin (Gibco) at 37 °C and 5% CO_2 in sterile conditions. PC12 pheochromocytoma cells (American Type Culture Collection #CRL-1721) were cultured with Ham's F12K medium (Sigma) supplemented with 15% horse serum, 2.5% fetal bovine serum and 1% penicillin–streptomycin. PC12 cells were primed with NGF (2.5S-NGF, Invitrogen) for 1 week before labeling experiments (50 ng/mL) and plated on substrates treated with poly-D-lysine hydrochloride (0.1 mg/mL) (Sigma, Mol. wt. >300,000).

Rat neonatal cortical (RNC) cells were obtained from decapitated 1–2 day old Sprague–Dawley rat pups. The cortex of the brain was transected, homogenized and incubated in Pronase solution (Calbiochem), followed by three cycles of centrifugation and trituration with meglumine buffer (2 μL of 0.5 M magnesium sulfate, 25 mg of *N*-methyl-glucamine, 0.6 mg of sodium chloride, 2.3 mg of HEPES and 1.7 mg of dextrose per mL of distilled, deionized water). Cells were resuspended in 1.5 mL of meglumine buffer and further triturated with flame-pulled, capillary pipettes. Cells were finally counted and plated at concentrations of 2×10^5 cells/cm in neurobasal medium (Gibco) with B-27 supplement (Gibco), glutamine (200 mM) and 1% penicillin–streptomycin. Substrates were previously coated with mouse laminin (3.03 μg/mL) (BDBiosciences) and poly-D-lysine hydrochloride (0.5 mg/mL).

2.4. Cell labeling

CdS qdots were separated from reaction subproducts by precipitation with the addition of 1-propanol (3 mL of 1-propanol/mL of nanocrystal solution). Similarly, MPA-coated CdTe qdots were precipitated with 2-propanol. The precipitate was isolated by centrifugation and dried in a vacuum oven for 1 h. The nanocrystals were resuspended in Dulbecco's PBS (D-PBS) (same volume as in the original solution) and sterile-filtered for conjugation with cells. Cells were placed on 22 mm × 22 mm no. 1 thickness coverslips using imaging chambers (Sigma, Cat. No. Z36,585-4) to retain fluid. Neuroblastoma and PC12 cells were cultured at densities of 1×10^4 cells/mL. After the cells reached ∼70% confluency (∼2 days), they were washed with D-PBS and blocked with 5% bovine serum albumin in D-PBS (BSA–DPBS,) for 1 h at 4 or 37 °C (endocytosis experiments). Following blocking, cells were washed with D-PBS and incubated with the qdot solution for 30 min at 4 or 37 °C. Finally, cells were washed two times with D-PBS, sealed in the imaging chambers using coverslips, and evaluated with fluorescence microscopy.

2.5. Characterization techniques

The nanocrystals were characterized by UV–vis absorbance and photoluminescence spectroscopy, high resolution transmission electron microscopy (HRTEM) and elemental analysis. Room temperature UV–vis absorbance spectra were obtained from aqueous dispersions using a Beckman DU500 spectrophotometer (Beckman Coulter, Fullerton, CA). HRTEM images of CdS qdots were obtained using a JEOL 2010F microscope operated with an accelerating voltage of 200 kV. For imaging, a drop of a dilute water dispersion of nanoparticles was dried on 200 mesh carbon-coated copper TEM grids (Electron Microscopy Sciences). Elemental analysis was carried out commercially at Desert Analytics, Tucson, Arizona, to determine cadmium and carbon content.

Fluorescence and phase contrast images of nerve cells were obtained using an Olympus IX70 inverted microscope with a mercury arc lamp and UV (λ_{exc} = 330–385) and narrowband green (λ_{exc} = 530–550) filter sets. Images were collected immediately after the incubation and washing of the qdot solutions, employing a 100× objective with oil immersion.

Fluorescence area quantitation was obtained using Adobe Photoshop to identify bright pixels and delineate selected areas of interest. The areas of qdot binding on the substrate and to the cells were both normalized by the total substrate area.

3. Results and discussion

3.1. Nonspecific binding

In a previous study, we created qdot bioconjugates with antibodies and specific peptide recognition sequences that bind to nerve cell integrin receptors [23]. Under certain conditions, nonspecific sticking of the nanocrystals to the cells reduced the ability to target effectively specific molecules on the cell surface. We found the nonspecific binding to be extremely sensitive to the nanocrystal synthesis conditions. For example, a difference in synthesis pH by a unit or two could lead to *extreme* differences in nonspecific binding, even when the cell labeling was performed under the same buffer conditions and nanocrystal concentrations, and the particles themselves were capped with the same ligand chemistry. To understand (and control) the effects of the synthetic conditions on nonspecific binding, cells were exposed systematically to nanocrystals produced at different reaction pH, capping ligand concentration and reactant molar ratio.

In reference [22], we studied the effect of the reaction parameters on the size and optical properties of the CdS

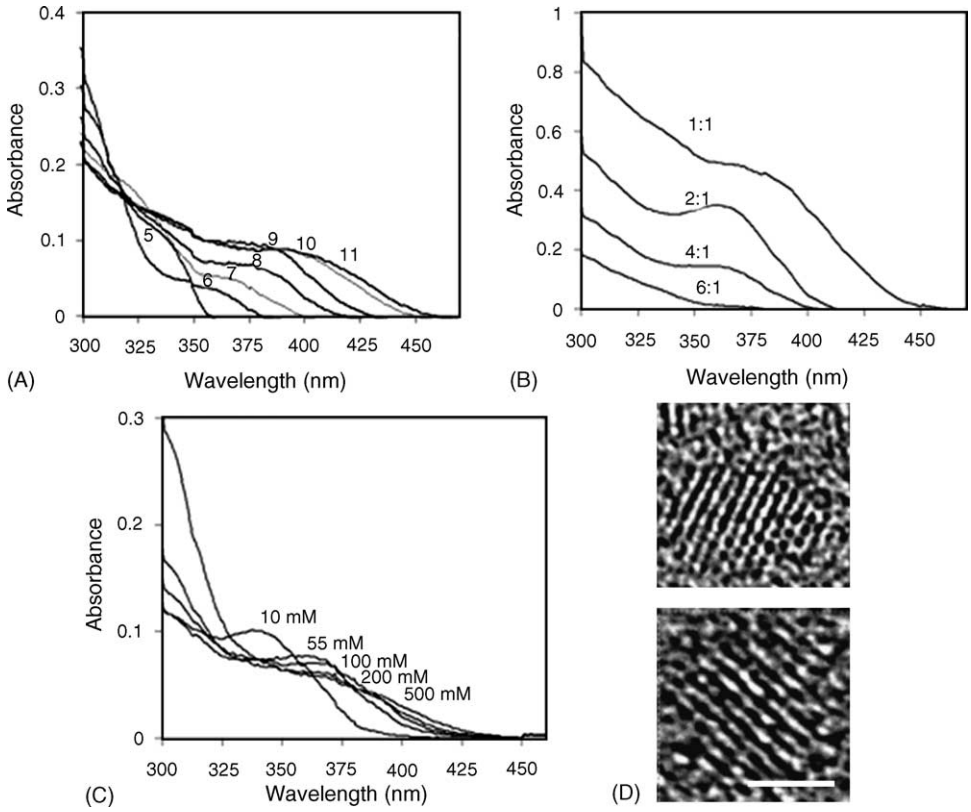

Fig. 1. UV–vis absorbance spectra and HRTEM of CdS quantum dots. Absorbance spectra of qdots synthesized with variation in (A) solution pH prior to Na_2S addition. (B) $[CdCl_2]$:$[Na_2S]$ molar ratio. (C) Concentration of MAA. (D) HRTEM images of CdS qdots synthesized at pH 7 (top panel) and pH 11 (bottom panel). The particle size can be tailored by adjusting any of these synthesis parameters, rendering larger particles with higher pH, lower $[CdCl_2]$:$[Na_2S]$ ratio and higher MAA concentration. Scale bar: 2 nm.

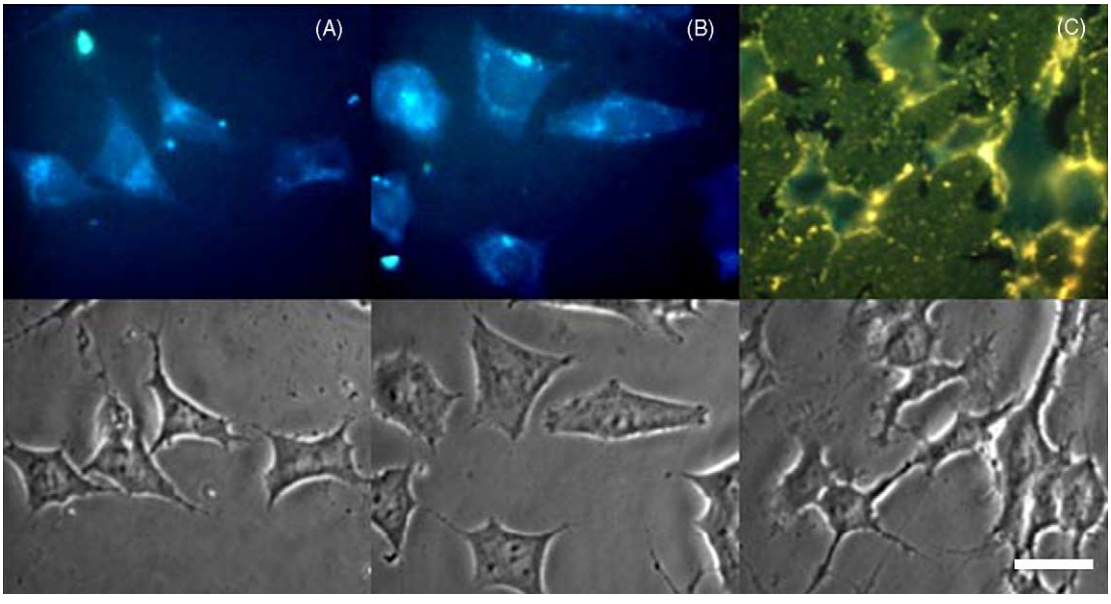

Fig. 2. Representative fluorescence and phase-contrast images of neuroblastoma cells nonspecifically labeled with CdS qdots synthesized at (A) pH 6, (B) pH 8, and (C) pH 11. The qdots were cleaned and resuspended in D-PBS (pH 7.4) prior to incubation with neuroblastoma cells at 4 °C for 30 min. The blue color corresponds to cellular autofluorescence. Scale bar: 25 μm. (For interpretation of the references to color in this figure legend, the reader is referred to the web version of the article.)

Table 2
Summary of CdS nanocrystal properties

Synthesis parameters[b]	Exciton peak absorbance wavelength (nm)	Diameter [c] (nm)
pH 5[a]	329	1.8
pH 7[a] (control)	357	2.3
pH 11[a]	388	3
$[CdCl_2]$:$[Na_2S]$ = 6:1	331	1.8
$[CdCl_2]$:$[Na_2S]$ = 1:1	378	2.8
[MAA] = 10 mM	338	1.9
[MAA] = 500 mM	370	2.6

[a] pH before Na_2S addition.
[b] All other parameters are the same as in the control synthesis.
[c] Determined from exciton peak absorbance [24].

nanocrystals. Fig. 1 provides a summary of CdS optical data with some representative HRTEM images of the nanocrystals. The correlation between the exciton peak energy and the particle size is well known for CdS and can be used to directly determine the average nanocrystal diameter from the optical measurements [24,25]. With increasing synthesis pH, the particle size increases, as revealed in the absorbance spectra in Fig. 1A with the exciton peak shifting to longer wavelength with higher synthesis pH (synthetic data is summarized in Table 2). To explore the effect of nanocrystal size on nonspecific binding, CdS nanocrystals were synthesized at different pH and then exposed to neuroblastoma cells at 4 °C. The optical fluorescence images in Fig. 2 and the calculated fluorescence areas (Fig. 6) reveal a strong correlation between the synthesis pH (presumably due to differences in nanocrystal size) and nonspecific binding (Fig. 2). Particles synthesized at pH 10 and 11 were largest and exhibited the greatest affinity for the cell membrane. Furthermore, these particles seemed to be extraordinarily adherent, as they bound uniformly not only to the cells, but also to the underlying substrate (Fig. 6).

Another route to changing the CdS nanocrystal size is to vary the $[CdCl_2]$:$[Na_2S]$ molar ratio while keeping the reaction pH the same. In these conditions, the nanocrystal diameter decreases as the $[CdCl_2]$:$[Na_2S]$ mole ratio decreases from 6:1 to 1:1 (Table 2). Fig. 3 shows fluorescence images of neuroblastoma cells exposed to the CdS nanocrystals at 4 °C. Again, the larger qdots exhibit much more nonspecific binding (quantitative data in Fig. 6) suggesting that the affinity for cell surfaces is greater for larger particles. *However*, nanocrystals synthesized with varying capping ligand concentrations produced different results.

Neuroblastoma cells were exposed at 4 °C to CdS qdots synthesized with varying MAA concentration, ranging from 10 to 500 mM. Higher ligand concentrations were found to produce larger nanocrystals. As shown in Fig. 4 and quantified in Fig. 6, all of the nanocrystals exhibited very little nonspecific binding (5–15% of cell or substrate area), regardless of the MAA concentration and corresponding nanocrystal diameter. Surprisingly, the qdots synthesized with 500 mM MAA, which are comparable in size to the particles used for labeling in Fig. 2C synthesized at pH 10 and 11, did not exhibit significant nonspecific binding.

The results in Fig. 4 indicate that particle-cell nonspecific binding depends not only on particle size, but also on the characteristics of the nanoparticle surface. Although the absorbance spectra provide information about the nanocrystal size, these measurements reveal nothing about differences in capping ligand surface coverage, which could be responsible for the observed differences in nonspecific binding.

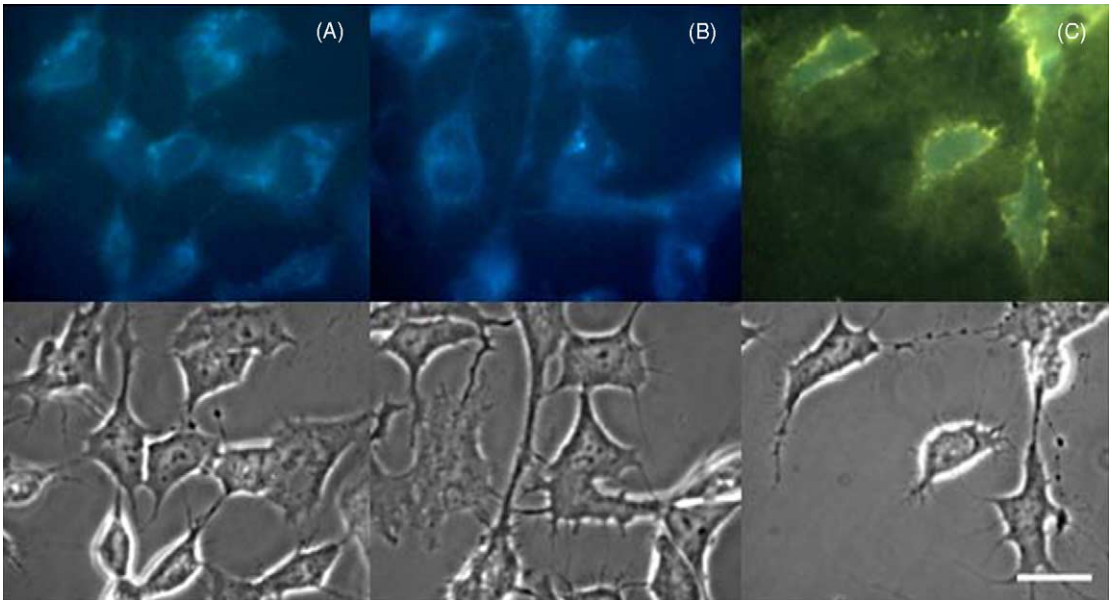

Fig. 3. Representative fluorescence and phase-contrast images of neuroblastoma cells nonspecifically labeled with CdS qdots synthesized at: (A) $[CdCl_2]$:$[Na_2S]$ = 6:1, (B) $[CdCl_2]$:$[Na_2S]$ = 4:1, and (C) $[CdCl_2]$:$[Na_2S]$ = 1:1. Qdots were cleaned and resuspended in D-PBS (pH 7.4) before incubation with neuroblastoma cells at 4 °C for 30 min. The blue color corresponds to cellular autofluorescence. Scale bar: 25 μm. (For interpretation of the references to color in this figure legend, the reader is referred to the web version of the article.)

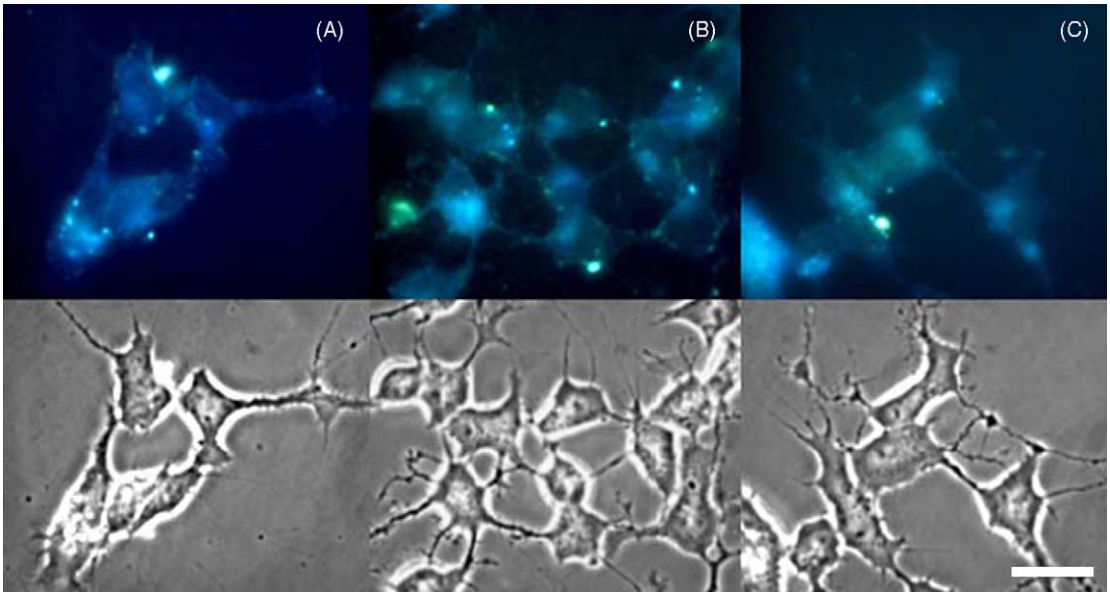

Fig. 4. Representative fluorescence and phase-contrast images of neuroblastoma cells nonspecifically labeled with CdS qdots synthesized with (A): [MAA] = 10 mM, (B) [MAA] = 100 mM, and (C) [MAA] = 500 mM. Qdots were cleaned and resuspended in D-PBS (pH 7.4) before incubation with neuroblastoma cells at 4 °C for 30 min. Scale bar: 25 μm.

Table 3
Elemental analysis and ligand coverage of representative CdS qdots

Synthesis parameters[b]	Cd atoms/qdot[c]	%Cd	%C	MAA molecules/qdot	MAA molecules/nm^2
pH 5[a]	62	38.72	8.90	66	6.50
pH 7[a] (control)	112	35.95	9.37	157	9.43
pH 11[a]	285	24.06	8.30	460	16.28[d]
[MAA] = 10 mM	72	38.51	8.76	77	6.80
[MAA] = 500 mM	165	34.34	8.23	208	9.80

[a] pH before Na_2S addition.
[b] All other parameters equivalent to the control synthesis.
[c] Determined from particle core diameter estimated from exciton peak energy in the absorbance spectra (Table 1) assuming bulk CdS density in the core.
[d] This high value was confirmed with two different measurements.

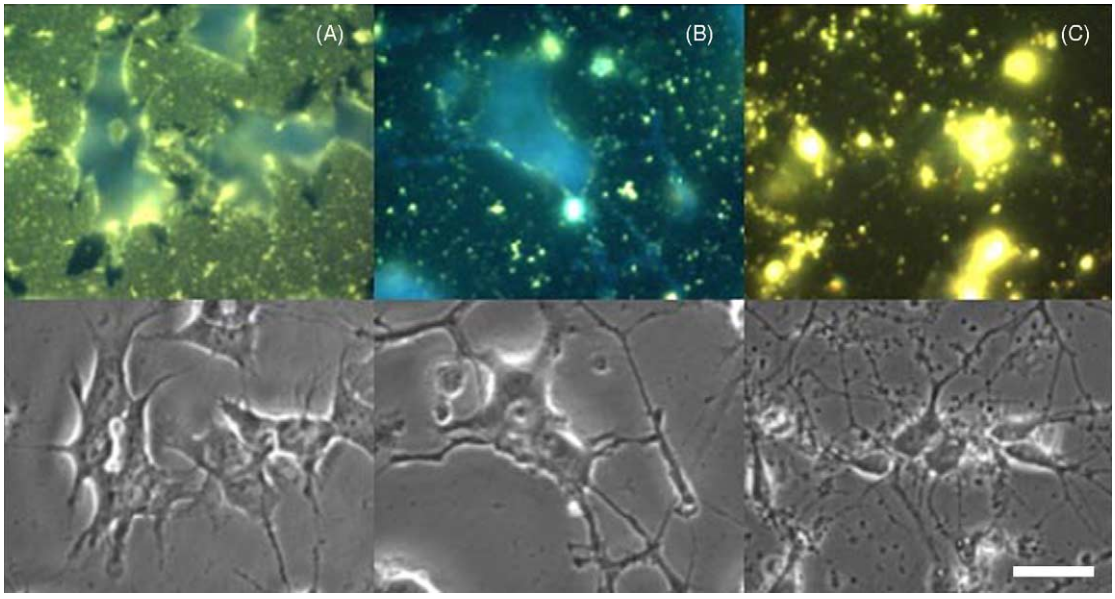

Fig. 5. Representative fluorescence and phase-contrast images of different cells types labeled with CdS qdots synthesized at pH 11 bound to (A) neuroblastoma cells, (B) PC12 cells, and (C) RNC cells. Qdots were cleaned and resuspended in D-PBS (pH 7.4) before incubation at 4 °C for 30 min. Scale bar: 25 μm.

Therefore, elemental analysis was performed to determine the capping ligand coverage of five different nanocrystal preparations, as summarized in Table 3. The ligand surface coverage was calculated from the measured Cd:C ratio and the average diameter determined from the exciton peak energy [25,26]. The number of Cd atoms per particle was estimated by assuming a bulk CdS density in the particle core. The primary difference between nanocrystals with a high degree of non-

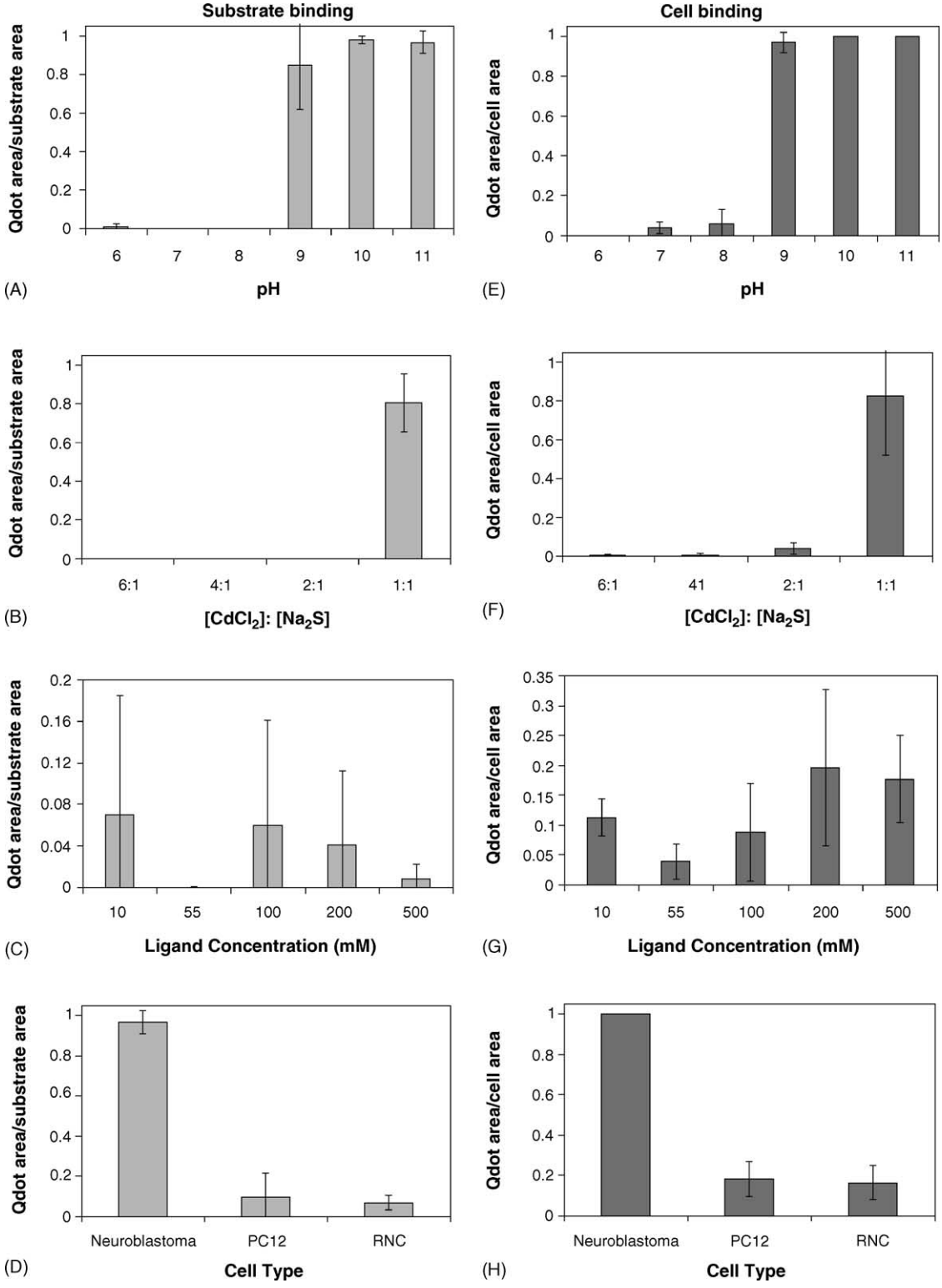

Fig. 6. Quantification of nonspecific CdS qdot binding to the substrate and cell surfaces. (A–D) Qdot-labeled substrate area per total substrate area with variation in: (A) solution pH prior to Na_2S addition, (B) $[CdCl_2]$:$[Na_2S]$ molar ratio, (C) concentration of MAA, (D) cell type. (E–H) Qdot-labeled cell area per total cell area with variation in (E) solution pH prior to Na_2S addition, (F) $[CdCl_2]$:$[Na_2S]$ molar ratio, (G) concentration of MAA, (H) cell type.

specific binding and those without appears to be the ligand surface coverage. The particles synthesized at pH 11 are coated with a much higher density of ligands than the particles of the same size synthesized with 500 mM MAA (but at pH 7). It is somewhat unexpected that the particles exhibiting the most nonspecific binding would have the highest ligand surface coverage since at physiological pH MAA is negatively charged and should be repelled by the negatively charged cell membrane. However, one should note that the ligand surface coverage for the qdots synthesized at pH 11 is even larger than the thiol ligand close-packed limit on the surface [40], indicating that excess ligands are somehow associated with the nanocrystal surface, which is perhaps the reason for increased nonspecific binding. For example, excess ligands on the nanocrystal surface could expose the sulfhydryl groups that would participate in cell binding. An excess of MAA might be caused by an incomplete purification and could be potentially remedied by improved separation processes such as electroelution [41].

Nonspecific binding of CdS nanocrystals was also examined on two other nerve cell types: rat PC12 and primary rat neonatal cortical (RNC) cells. Nanocrystals synthesized at pH 11 ([MAA] = 55 mM) were used as a model system since they exhibited substantial nonspecific binding to the neuroblastoma cells. Fig. 5 shows significant differences in nonspecific binding to the different cell types. As shown above, nonspecific binding to neuroblastoma cells is pervasive, exhibiting attachment to the substrate as well. Nonspecific binding was substantially less for PC12 cells and somewhat less for RNC cells as quantified in Fig. 6. In both cases, nanocrystals were not found attached to the substrate significantly. The differences in nonspecific binding may be related to the medium used for culturing the cells: the neuroblastoma cells are grown on glass coverslips without a coating and the culture medium contains less serum in comparison to the medium used for PC12 and RNC cells. Serum proteins likely adsorb on the substrate, which could potentially prevent nanocrystal adsorption. Another significant difference between cell types could relate to the cell membrane composition and the excreted extracellular matrix (ECM) components. The ratios of lipids, glycolipids, gangliosides and membrane proteins often vary with factors such as culture substratum, developmental stage, cell density and differentiation [28–31]. In particular, lipid composition has

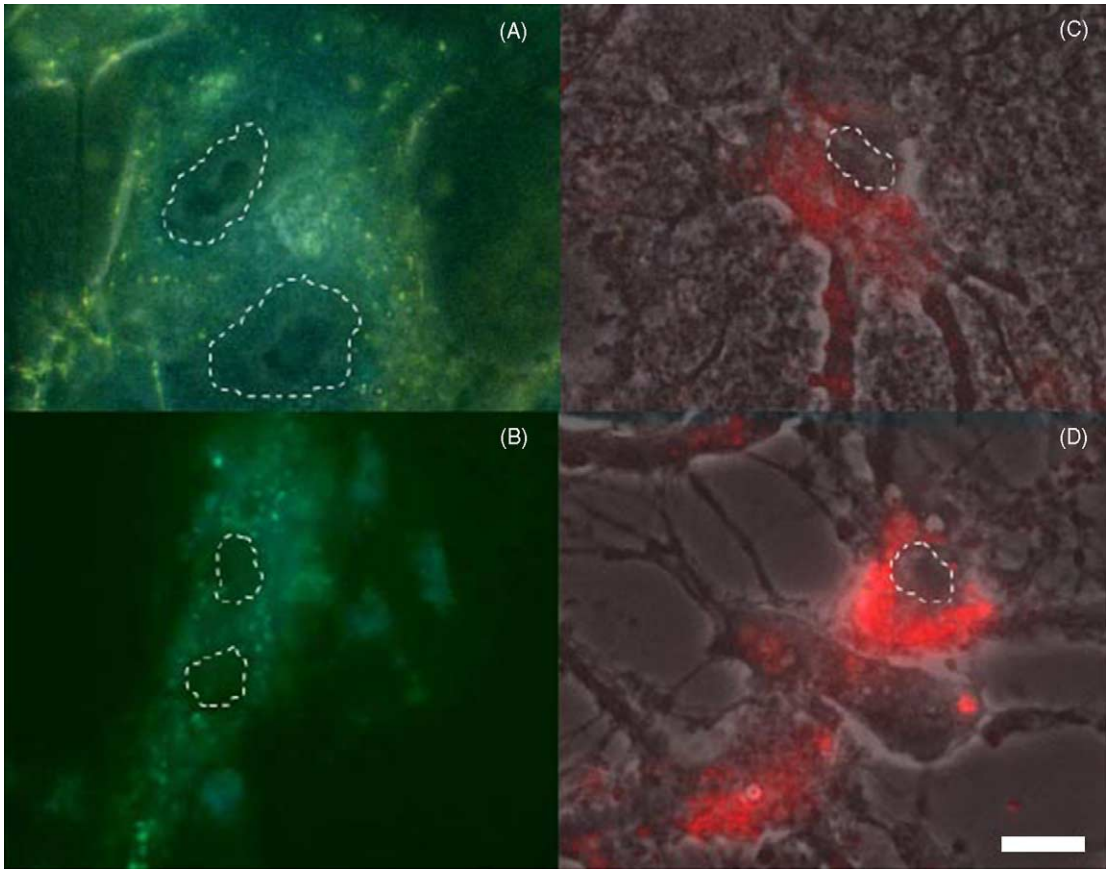

Fig. 7. Representative images (combined fluorescence and phase-contrast images) showing endocytosis of qdots. (A) Neuroblastoma cells nonspecifically labeled at 37 °C with CdS qdots synthesized at pH 11. (B) Neuroblastoma cells with peptide-directed labeling at 37 °C using MAA-RGD CdS qdots. (C) RNC cells nonspecifically labeled at 37 °C with MPA-CdTe qdots. (D) RNC cells specifically labeled at 37 °C with MPA-RGD CdTe qdots. Qdots were cleaned and resuspended in D-PBS (pH 7.4) before incubation with cells at 37 °C for 30 min. Qdots were exclusively present in the cytoplasm and the perinuclear region. The dotted lines delineate the cell nuclei. Scale bar: 10 μm.

been reported to play a fundamental role in binding to extracellular compounds. For example, a significant increase in binding to calcium oxalate crystals was observed when the cellular lipid composition was selectively altered by increasing negatively charged phosphatidylserine [32].

3.2. Nanocrystal endocytosis

Endocytosis, the natural recycling of the cell membrane, occurs with relatively high rates and makes it generally necessary to carry out in vitro cellular membrane labeling in living cells with fluorescent probes at 4 °C to suppress the metabolic processes in the cells and reduce endocytosis [11,33]. However, for active stimulation and also for in vivo experiments of cells, it is essential to maintain cells at physiological temperature to guaranty normal cell function and responses to external stimuli. Although endocytosis has been widely examined at larger length scales [39], there is almost no data on the rates of endocytosis of nanocrystals smaller than 10 nm attached to cell membranes at physiological temperatures. We observed rapid nanocrystal endocytosis at 37 °C, regardless of the surface chemistry, the cell type, or qdots employed (Fig. 7). For example, we investigated CdS particles bound to neuroblastoma cells with both nonspecific MAA coatings and peptide-recognition fragments. Qdot endocytosis occurs nearly instantaneously, and within ∼5 min the nanocrystals are internalized, as shown in Fig. 7A and B. RNC cells exhibited the same rapid endocytosis of MAA-coated and peptide-tagged CdTe nanocrystals, as shown in Fig. 6C and D.

The observation of nanocrystal endocytosis is consistent with previous observations of endocytosis of qdots attached to cell surfaces at physiological temperature both nonspecifically [11,14,33,34] and via specific cell surface receptors [2,10,35]. However, in the vast majority of these studies, endocytosis was desired, for example providing an endosome marker [34], allowing observation of phagokinetic tracks [14], or enhancing the understanding of signal transduction [35]. Clearly, endocytosis is a major obstacle to creating stable long-term active qdot-cell interfaces with membrane receptors.

4. Conclusions

In conclusion, active interfacing between cells and quantum dots faces many challenges. We have highlighted here two major challenges – nonspecific binding and endocytosis – found to occur using MAA-CdS nanoparticles, which represent a simple model system for evaluating qdots with thin molecular coatings of the type needed for electro-active stimulation of cells. While applications involving passive qdot-cell interfaces, such as imaging, can use thick surface coatings of molecules like PEG to prevent nonspecific binding and endocytosis [6–10], this coating is too insulating to enable *active* qdot-cell interfaces and alternative strategies are required. It appears that nonspecific binding can be alleviated with judiciously chosen synthetic conditions and capping ligands. Endocytosis at physiological temperatures, however, will be difficult to avoid. Targeting receptors on the membrane surface that are not continuously recycled could potentially alleviate this problem, but this approach limits nanocrystal targeting to only a handful of receptors. Perhaps a limited number of PEG molecules on the nanocrystal surface would be sufficient to prevent endocytosis without disrupting the potential for communication between the qdot and the cell surface. In fact, a controlled synthesis of particles with only a few molecules of PEG on a nanocrystal surface has been reported [7], and the adaptation of such a process could potentially offer a viable strategy for active qdot-cell interfacing without the problems of nonspecific binding and endocytosis. Other potential solutions include the development of hydrophilic organic dendrons as ligands, which could produce a thin (1–2 nm) tightly-packed shell that protects the nanocrystal core and allows surface modification as well [36]. Also, chelating ligands incorporating carbodithioates could be designed to enhance photo-stability and include tailored segments for cellular interactions [37]. In addition, these new strategies could help overcome other challenges such as cytotoxicity [12], which we have also observed particularly with RNC cells and CdTe qdots.

Acknowledgements

Funding for this work was provided by the Texas Higher Education Coordinating Board through their ARP Program (CES, BAK), an NSF NER Grant (BES 0303442, CES, BAK), an NSF graduate research fellowship (JOW), and the NSF IGERT program (JOW).

References

[1] M. Bruchez Jr., M. Moronne, P. Gin, S. Weiss, A.P. Alivisatos, Science 281 (1998) 2013.
[2] W.C. Chan, S. Nie, Science 281 (1998) 2016.
[3] X. Wu, H. Liu, J. Liu, K.N. Haley, J.A. Treadway, J.P. Larson, N. Ge, F. Peale, M.P. Bruchez, Nat. Biotechnol. 21 (2001) 41.
[4] F. Chen, D. Gerion, Nano Lett. 4 (2004) 1827.
[5] M.E. Akerman, W.C. Chan, P. Laakkonen, S.N. Bhatia, E. Ruoslahti, PNAS 99 (2002) 12617.
[6] B. Dubertret, P. Skourides, D.J. Norris, V. Noireaux, A.H. Brivanlou, A. Libchaber, Science 298 (2002) 1759.
[7] X. Gao, Y. Cui, R.M. Levenson, L.W. Chung, S. Nie, Nat. Biotechnol. 22 (2004) 969.
[8] B. Ballou, B.C. Lagerholm, L.A. Ernst, M.P. Bruchez, A.S. Waggoner, Bioconjug. Chem. 15 (2004) 79.
[9] H. Xu, F. Yan, E.E. Monson, R. Kopelman, J. Biomed. Mater. Res., 66A (2003) 870.
[10] A.M. Derfus, W.C. Chan, S.N. Bhatia, Adv. Mater. 16 (2004) 961.
[11] A. Hoshino, K. Hanaki, K. Suzuki, K. Yamamoto, Biochem. Biophys. Res. Commun. 314 (2004) 46.
[12] A.M. Derfus, W.C. Chan, S.N. Bhatia, Nano Lett. 4 (2004) 11.
[13] S. Wang, N. Mamedova, N.A. Kotov, W. Chen, J. Studer, Nano Lett. 2 (2002) 817.

[14] W.J. Parak, R. Boudreau, M.L. Gros, D. Gerion, D. Zanchet, C.M. Micheel, S.C. Williams, A.P. Alivisatos, C. Larabell, Adv. Mater. 14 (2002) 882.
[15] D. Gerion, F. Pinaud, S.C. Williams, W.J. Parak, D. Zanchet, S. Weiss, A.P. Alivisatos, J. Phys. Chem. B 105 (2001) 8861.
[16] M. Green, Angew. Chem. Int. Ed. 43 (2004) 4129.
[17] A.P. Alivisatos, Science 271 (1996) 933.
[18] V.L. Colvin, A.P. Alivisatos, J. Chem. Phys. 97 (1992) 730.
[19] C. Loo, A. Lin, L. Hirsch, M.H. Lee, J. Barton, N. Halas, J. West, R. Drezek, Tech. Cancer Res. Treat. 3 (2004) 33.
[20] R. Bakalova, H. Ohba, Z. Zhelev, T. Nagase, R. Jose, M. Ishikawa, Y. Baba, Nano Lett. 4 (2004) 1567.
[21] D. Ishii, K. Kinbara, Y. Ishida, N. Ishii, M. Okochi, M. Yohda, T. Aida, Nature 423 (2003) 628.
[22] J.O. Winter, N. Gomez, S. Gatzert, C.E. Schmidt, B.A. Korgel, Colloids Surf. A 254 (2005) 147.
[23] J.O. Winter, T.Y. Liu, B.A. Korgel, C.E. Schmidt, Adv. Mater. 13 (2001) 1673.
[24] W.W. Yu, L. Qu, W. Gao, X. Peng, Chem. Mater. 15 (2003) 2854.
[25] T. Vossmeyer, L. Katsikas, M. Giersig, I.G. Popovic, K. Diesner, A. Chemseddine, A. Eychmuller, H. Weller, J. Phys. Chem. 98 (1994) 7665.
[26] Ch. Barglik-Chory, D. Buchold, M. Schmitt, W. Kiefer, C. Heske, C. Kumpf, O. Fuchs, L. Weinhardt, A. Stahl, E. Umbach, M. Lentze, J. Geurts, G. Muller, Chem. Phys. Lett. 379 (2003) 443.
[27] S.J. Rosenthal, I. Tomlinson, E.M. Adkins, S. Schroeter, S. Adams, L. Swafford, J. McBride, Y. Wang, L.J. DeFelice, R.D. Blakely, J. Am. Chem. Soc. 124 (2002) 4586.
[28] I. Lelong, E. Frechard, G. Cremel, K. Langley, G. Rebel, G. Vincendon, M. Mersel, Dev. Neurosci. 13 (1991) 54.
[29] C. Schengrund, M.A. Repman, J. Neurochem. 39 (1982) 940.
[30] D. Glyn, J. Biol. Chem. 254 (1979) 155.
[31] T.H. Young, C.H. Hung, J. Biomed. Mater. Res. Part A 67A (2003) 1238.
[32] M.W. Bigelow, J.H. Wiessner, J.G. Kleinman, N.S. Mandel, Am. J. Physiol. 272 (1997) 55.
[33] J.K. Jaiswal, H. Mattoussi, J.M. Mauro, S.M. Simon, Nat. Biotechnol. 21 (2003) 47.
[34] K. Hanaki, A. Momo, T. Oku, A. Komoto, S. Maenosono, Y. Yamaguchi, K. Yamamoto, Biochem. Phys. Res. Commun. 302 (2003) 496.
[35] D. Lidke, P. Nagy, R. Heintzmann, D.J. Arndt-Jovin, J.N. Post, H.E. Grecco, E.A. Jares-Erijman, T.M. Jovin, Nat. Biotechnol. 22 (2004) 198.
[36] Y.A. Wang, J.J. Li, H. Chen, X. Peng, J. Am. Chem. Soc. 124 (2002) 2293.
[37] C. Querner, P. Reiss, J. Bleuse, A. Pron, J. Am. Chem. Soc. 126 (2004) 11574.
[38] F. Osaki, T. Kanamori, S. Sando, T. Sera, T. Aoyama, J. Am. Chem. Soc. 126 (2004) 6520.
[39] I. Pastan, M.C. Willingham (Eds.), Endocytosis, Plenum Press, New York, 1985.
[40] B.A. Korgel, S. Fullam, S. Connolly, D. Fitzmaurice, J. Phys. Chem. B 102 (1998) 8379.
[41] D.A. Heller, R.M. Mayrhofer, S. Baik, Y.V. Grinkova, M.L. Usrey, M.S. Strano, J. Am. Chem. Soc. 126 (2004) 14567.